3-2018

Crystal Structure and Computational Analysis of a Two-Dimensional Coordination Polymer, BiI3(DppeO2)3/2

Andrew W. Kelly

Amelia M. Wheaton

Aaron D. Nicholas

Howard H. Patterson

Robert D. Pike

Crystal Structure and Computational Analysis of a Two-dimensional Coordination Polymer, $BiI_3(DppeO_2)_{3/2}$

Andrew W. Kelly,[a] Amelia M. Wheaton,[a] Aaron D. Nicholas,[b] Howard H. Patterson,[b] and Robert D. Pike[a]*

[a]*Department of Chemistry, College of William and Mary, Williamsburg, VA 23187.*

[b]*Department of Chemistry, University of Maine, Orono, ME 04469-5706.*

Corresponding Author: Robert D. Pike

Department of Chemistry

College of William and Mary

Williamsburg, VA 23187-8795.

telephone: 757-221-2555

FAX: 757-221-2715

email: rdpike@ wm.edu

X-ray crystal structure; bismuth(III); coordination polymer; phosphane oxide; DFT calculations

Abstract:

Catena-poly[*fac*-triiodobismuth(III)-tris-(μ-ethane-1,2-diylbis(diphenylphosphane oxide-κ^2O,O'))], a 2-D sheet network of BiI_3 was synthesized from BiI_3 and ethane-1,2-diylbis(diphenylphosphane oxide ($DppeO_2$) in tetrahydrofuran. The crystal structure revealed a trigonal structure with three-fold symmetry at Bi. Bismuth centers show *fac*-BiI_3O_3 coordination, with Bi–I = 2.9416(2) Å and Bi–O = 2.4583(17) Å. The I–Bi–I and O–Bi–O angles (95.520(7)° and 79.04(6)°, respectively) indicate trigonal distortion in the Bi octahedron. Bridging $DppeO_2$ ligands centered on inversion centers give rise to a 2-D sheet polymer. The 8.3 Å thick sheets consist of three layers in a sandwich structure. The outer layers are composed of phenyl rings and BiI_3 groups with the iodide atoms pointing outward. The central layer consists of the $O{=}PCH_2CH_2P{=}O$ bridging groups. Computational results suggest that semi-conducting behavior arises from Bi(III) centers. A halide to $DppeO_2$ π^* transition is suggested by theoretical results.

Introduction:

Despite its placement amongst the heavy metals, Bi is widely regarded as non-toxic. Bismuth(III) halides systems are of interest because they represent precursors for, or alternatives to, BiOX photocatalysts (X = Cl, Br, I) [1]-[4]. Bismuth(III) oxyhalides have relatively low energy band gap values 3.22, 2.64, and 1.77 eV for X = Cl, Br, and I, respectively [5]. The bismuth(III) center in BiOX has been shown to be a source of hole-electrons when irradiated in the near-UV or visible range [2],[5],[6]. The resulting radicals, such as hydroxide or superoxide, have been demonstrated to cause the destruction of organic pollutants in comparable fashion to that of TiO_2. Precursor or alternative complexes to BiOI would ideally contain the elements Bi, O, and I. Nevertheless, relatively few molecular or network species of this composition are known. Thus, we set out to produce a network containing BiI_3 bridged by oxygen-containing bridging ligands.

Bismuth(III) halides readily form a wide variety of ionic and neutral clusters [7]-[10]. These have been shown to be readily capped by oxygen donors such as hexamethylphosphoramide (hmpa), dimethyl sulfoxide (dmso), triphenylphosphane oxide (PPh_3O), triphenylarsane oxide ($AsPh_3O$), tetrahydrofuran (THF), and various polyethers [11]-[17]. As with all 6-coordinate Bi(III) complexes, the products of these reactions feature essentially octahedral Bi centers, and in some cases also show bridging halide centers. For example, $Bi_2I_6(PPh_3O)_4$ is an iodide-bridged dimer and $Bi_2I_6(hmpa)_2$ is an iodide-bridged polymer chain, whereas $[BiI_2(hmpa)_4]^+$ is monomeric. Molecular $BiX_3(LL)$ complexes (X = Cl, Br, I) have been prepared in which LL = $(^{i}PrO)_2(O)PCH_2P(O)(O^{i}Pr)_2$ is chelating [18]. Coordination polymers of Bi not linked via bridging halides are very rare. A single report involving bridging oxygen donors utilizes aryl di- and triphosphonic acid esters, such as 4,4'-$[(^{i}PrO)_2P(O)]C_6H_4C_6H_4[P(O)(O^{i}Pr)_2]$ [19]. These bridging ligands resulted in formation of 1- and 2-D polymers of BiX_3.

The structurally dependent bismuth-halide band gap has been shown to play a pivotal role in the photochemical and photophysical properties of these systems including photo- and thermochromic

behavior [10],[20-21]. Early examples include the thermochromic changes in 1,10-phenanthrolinium salts of $[BiI_4]^-$ studied by Tershansy *et al*. [22]. These brightly colored crystals blue shift upon cooling from 296 K to 100 K. Temperature-dependent XRD studies reveal that changes to the Bi–I and Bi···Bi distances are responsible for this photophysical change. Our recent work on related iodobismuthate(III) complexes has also added to the understanding of these systems [23]. However, despite reported studies of bismuth(III)-containing halide crystals, the photophysical properties of these systems remain difficult to predict.

Here we report the preparation of $BiI_3(DppeO_2)_{3/2}$ (**1**, $DppeO_2$ = ethane-1,2-diylbis(diphenylphosphane oxide)), representing only the second instance of an oxygen-ligand-bridged bismuth(III) iodide polymer, following $[(BiI_3)_2(4,4'\text{-}[(^iPrO)_2P(O)]C_6H_4C_6H_4[P(O)(O^iPr)_2])]\bullet¼CH_3CN$ [19]. Due to the presence in **1** of an isolated metal-halide center with coordinated aromatic ligands, a number of possible electronic transitions are possible. Thus, density functional theory (DFT) and time-dependent (TD-DFT) calculations have been performed to predict and visualize the electronic transitions in **1** upon photo irradiation. We believe our findings contribute to the theoretical understanding of the photochemical and photophysical properties of oxygen-ligand-bridged bismuth(III) halide polymers.

Experimental:

General:

BiI_3 and 1,2-bis(diphenylphosphanyl)ethane (Dppe) were obtained from Sigma-Aldrich and were used as received. Ethane-1,2-diylbis(diphenylphosphane oxide) ($DppeO_2$) was prepared by H_2O_2 oxidation of Dppe following the literature [24]. Acetone was distilled from Drierite and tetrahydrofuran (THF) was purified using an LC Technologies SPBT-1 bench top solvent purifier. Analysis for C and H was carried out by Atlantic Microlabs, Norcross, GA. Thermogravimetric analyses (TGA) were conducted using a TA Instruments Q500 in the dynamic (variable temp.) mode with a maximum heating rate of 50 ^oC/min. to 800 ^oC under 60 mL/min. N_2 flow.

*Synthesis of **1**:*

BiI_3 (176 mg, 0.298 mmol) was dissolved in 10 mL THF to form a yellow solution. $DppeO_2$ (215 mg, 0.500 mmol) was dissolved in 10 mL warm THF to form a colorless solution. The solutions were combined and stirred for 12 hours under air, during which time a yellow precipitate formed. The solid was collected by vacuum filtration and dried under vacuum (292 mg, 0.236 mmol, 79.3%). Anal. Calcd for $C_{39}H_{36}BiI_3O_3P_3$: C, 37.92; H, 2.94. Found: C, 37.65; H, 3.09.

X-ray crystallography:

Crystals were grown from an acetone solution of **1**, which was layered with ethyl ether in 5 mm i.d. tubes. A selected crystal was mounted on a glass fiber. All measurements were made using graphite-monochromated Mo Kα radiation on a Bruker-AXS three-circle DUO diffractometer, equipped with a SMART Apex II CCD detector. Initial space group determination was based on a matrix consisting of 36 frames. The data were reduced using SAINT+ [25], and empirical absorption correction applied using SADABS [26].

The structure was solved using intrinsic phasing. Least-squares refinement was carried out on F^2. The non-hydrogen atoms were refined anisotropically. Hydrogen atoms were placed in riding positions and refined isotropically. Structure solution, refinement, and the calculation of derived results were performed using the SHELXTL package of computer programs [27] and ShelXle [28]. Details of the X-ray experiment and crystal data are summarized in Table 1. Selected bond lengths and bond angles are given in Figure 2.

Computational Details:

The empirical formula of **1** contains a fractional amount of $DppeO_2$ (3/2). In order to perform DFT and TD-DFT calculations on **1**, we developed a model with the formula $BiI_3(DppeO_2)_3$ that would preserve the octahedral geometry of the Bi(III) center, Scheme 1. Density functional theory (DFT) calculations at the B3LYP level of theory using the SDD basis set as implemented in the Gaussian 09 software was used for all atoms [29-32]. Ground state geometry parameter results agree with the experimental XRD data described below. Because of its agreement to the experimental data, we used this ground state geometry for molecular orbital (MO) calculations and performed TD-DFT calculations all at the B3LYP level of theory using the SDD basis set for all atoms [33-35]. MOs were generated and visualized using the Avogadro 1.2.0 software program [36].

Scheme 1. DFT model of formula $BiI_3(DppeO_2)_3$ used in the calculations of **1**.

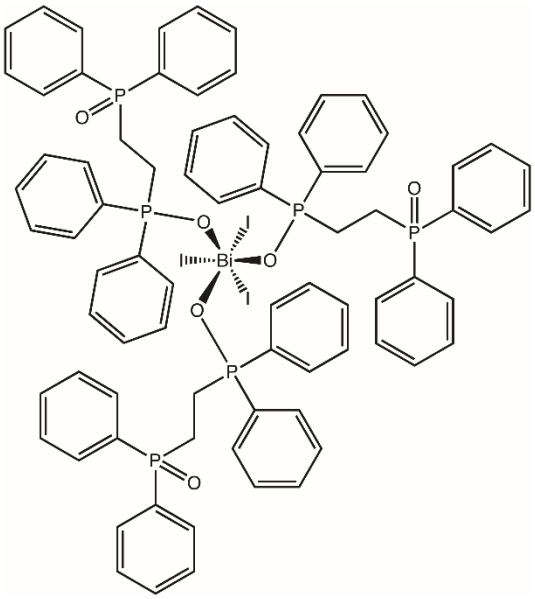

Results and Discussion:

Synthesis and Structure:

The title compound, $BiI_3(DppeO_2)_{3/2}$ (**1**), was easily prepared by reacting BiI_3 and $DppeO_2$ in THF solution. The product slowly forms from solution as a yellow powder in good yield. Elemental analysis and

thermogravimetric analysis (TGA) confirmed that **1** consists of a 2:3 ratio of BiI_3 and $DppeO_2$. The TGA trace revealed a sharp loss in mass between 295 and 350 °C, corresponding to the loss of all ligands, and leaving Bi, 19.4% remaining mass (theoretical = 16.9%, see Figure 1). Recrystallization of **1** from acetone/ethyl ether produced orange crystals that solved in trigonal space group R–3c.

Figure 1. TGA trace of $BiI_3(DppeO_2)_{3/2}$, **1**.

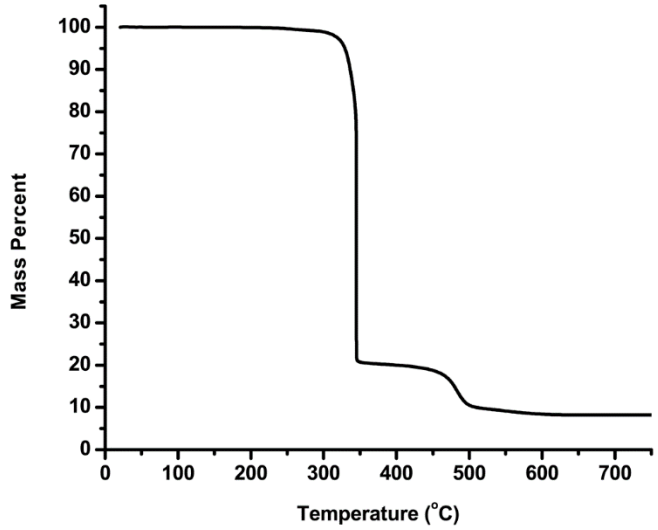

The crystallographically independent unit of **1** consists of $Bi_{1/3}I(DppeO_2)_{1/2}$ (Figure 2). The Bi atom lies on a 3-fold rotation center, and the ethane group of $DppeO_2$ is centered on an inversion center. Bond lengths and angles in **1** are unexceptional. Trigonal distortion from octahedral geometry about Bi is evident from the relatively large I–Bi–I bond angle (95.520(7)°) and small O–Bi–O bond angle (79.04(6)°).

Figure 2. Thermal ellipsoid drawing of $BiI_3(DppeO_2)_{3/2}$, **1**. Displacement ellipsoids shown at 50% probability. Hydrogen atoms are omitted. Color scheme for Figures 2–6: Bi orange, I purple, O red, P pink, C grey. Selected bond lengths (Å) and angles (°): Bi1–O1 2.4583(17), Bi1–I1 2.9416(2), P1–O1 1.4980(19), O1–Bi1–O1’ 79.04(6), O1–Bi1–I1 163.19(4), O1’–Bi1–I1 84.50(4), O1”–Bi1–I1 101.21(4), I1–Bi1–I1’ 95.520(7). Symmetry transformations used to generate equivalent atoms: ’ –x+y+1,–x+1,z; ” –y+1,x–y,z.

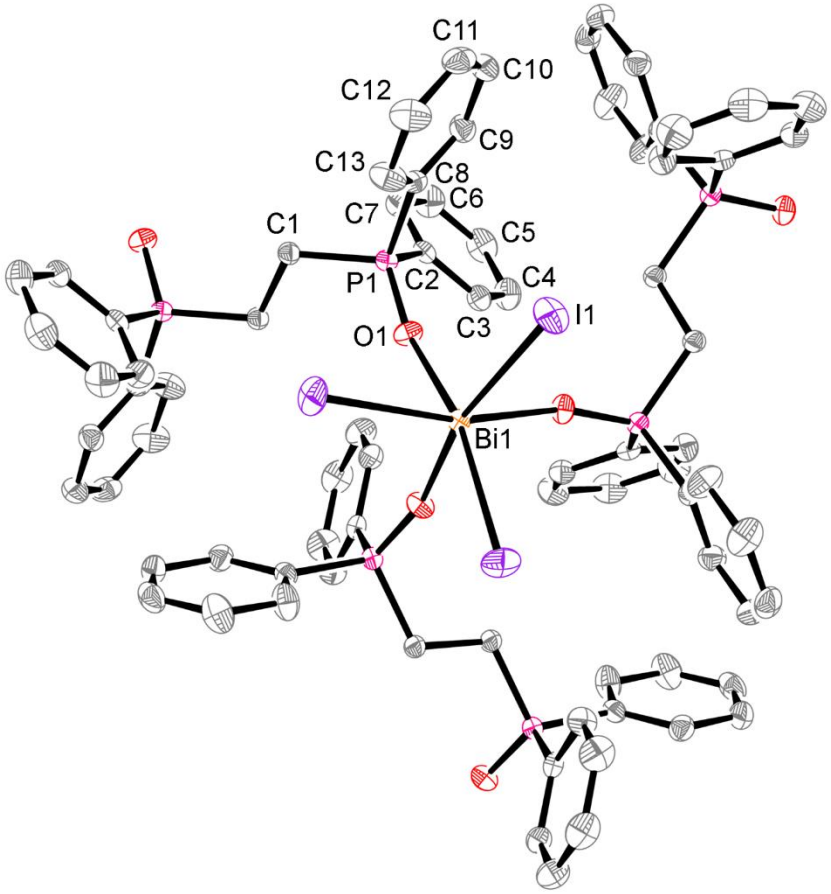

Compound **1** is the first example of a diphosphane dioxide coordination polymer of Bi. Expansion of **1** via special positions produces a 2-D coordination polymer (Figure 3). The 2-D sheet, which is nearly perfectly planar, is about 8.3 Å thick (Figure 4). *fac*-BiI_3 units alternate between sheet faces, as do the phenyl rings. Thus, the sheet consists of three layers, with the two outer BiI_3/phenyl layers surrounding a central layer of $OPCH_2$ units (Figure 4).

Figure 3. Ball and stick packing diagram of $BiI_3(DppeO_2)_{3/2}$, **1**, projected perpendicular to *c*-axis, showing network formation. Carbon atoms are shown as capped sticks; hydrogen atoms are omitted.

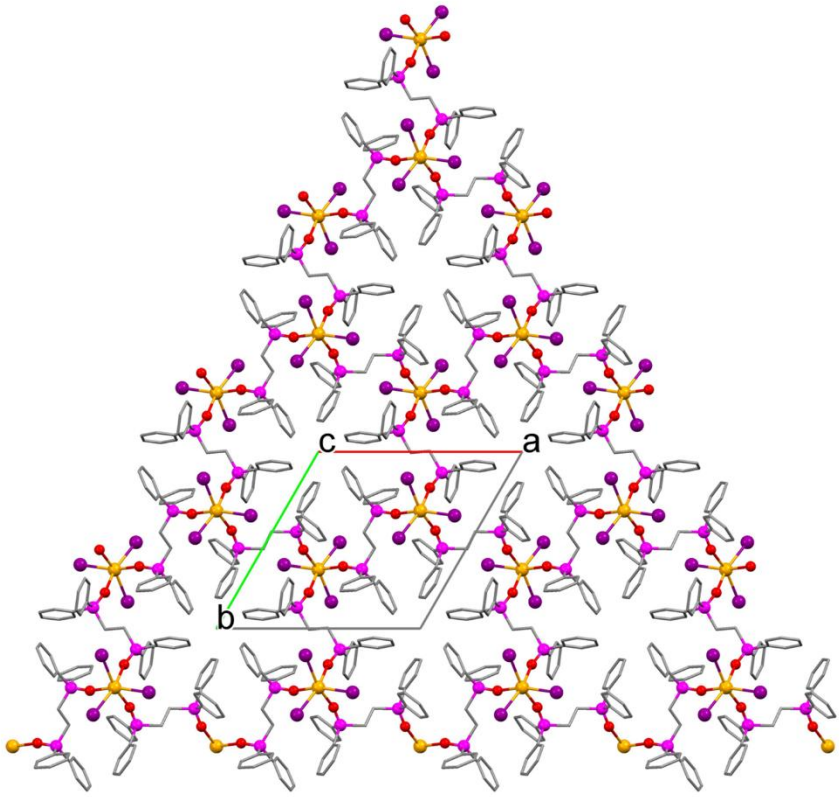

Figure 4. Space-filling diagram of **1** projected perpendicular to *a*-axis showing 2-D sheet structure. Hydrogen atoms are omitted.

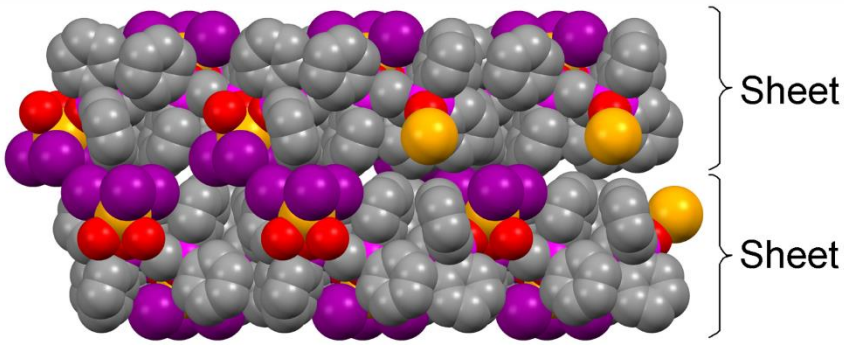

DFT and TD-DFT Calculations

Our group and others have reported on the various electronic transitions bismuth(III) iodide complexes undergo upon excitation, which include ligand-to-metal charge transfer (LMCT), mixed halide/metal-to-ligand charge transfer (X/MLCT), and cluster-centered metal halide rearrangement (CC)

[23],[37-42]. The high degree of conjugation in the $DppeO_2$ ligand further offers the possibility of ligand $\pi \rightarrow \pi^*$ transitions in **1** [37],[38]. The wide variety of transitions reported in BiI_3 complexes makes it difficult to predict the nature of the transitions in **1**. To investigate this question, we employed DFT calculations on a model of **1** with molecular formula $BiI_3(DppeO_2)_3$ (Scheme 1). Ground state calculation results are shown in Figure 5 and summarized in Table 2. Ground state parameters are in general agreement with experimental X-ray structural values (Table 2). Minor deviations between experimental and calculated Bi–O and Bi–I bond lengths were observed in the quasi-octahedral bond angles. We attribute these minor structural differences to the fact that these calculations are performed in the gas phase, allowing for a higher degree of rotational and translational freedom, but failing to account for packing effects present in a solid crystalline state.

Figure 5. DFT ground state geometry for the $BiI_3(DppeO_2)_3$ unit.

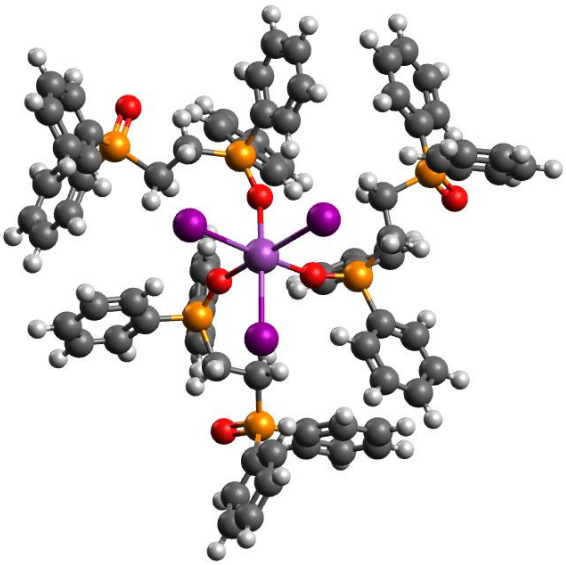

Molecular orbital calculations for the ground state (Figure 6) show that the higher occupied molecular orbitals are composed of the Bi 6s and I 5p atomic orbitals. The lower unoccupied molecular orbitals are composed of the ligand π^* orbitals. This MO composition is not surprising given other reports

of bismuth(III) iodide complexes containing aromatic ligands [37]-[42]. In these systems, the higher molecular orbitals have also been localized to the iodobismuth(III) center, while the lower unoccupied molecular orbitals are localized to aromatic ligands. Given this MO composition and the lack of evidence for π stacking interaction in the X-ray structure, it is unlikely that any $\pi \rightarrow \pi^*$ transition occurs upon photoexcitation. MO calculations do not predict any energetically-accessible unoccupied MOs consisting of the Bi 6p AOs. This eliminates the possibility of a metal-halide cluster rearrangement during excitation. Rather, what is occurring in **1** is most likely an X/MLCT or XLCT transition.

Figure 6. DFT calculated frontier orbitals of $BiI_3(DppeO_2)_3$ in the ground state showing the HOMO-3 through LUMO+3. The HOMOs are composed primarily of the I 5p and Bi 6s atomic orbitals, while the LUMOs are composed of the $DppeO_2$ π^* orbitals.

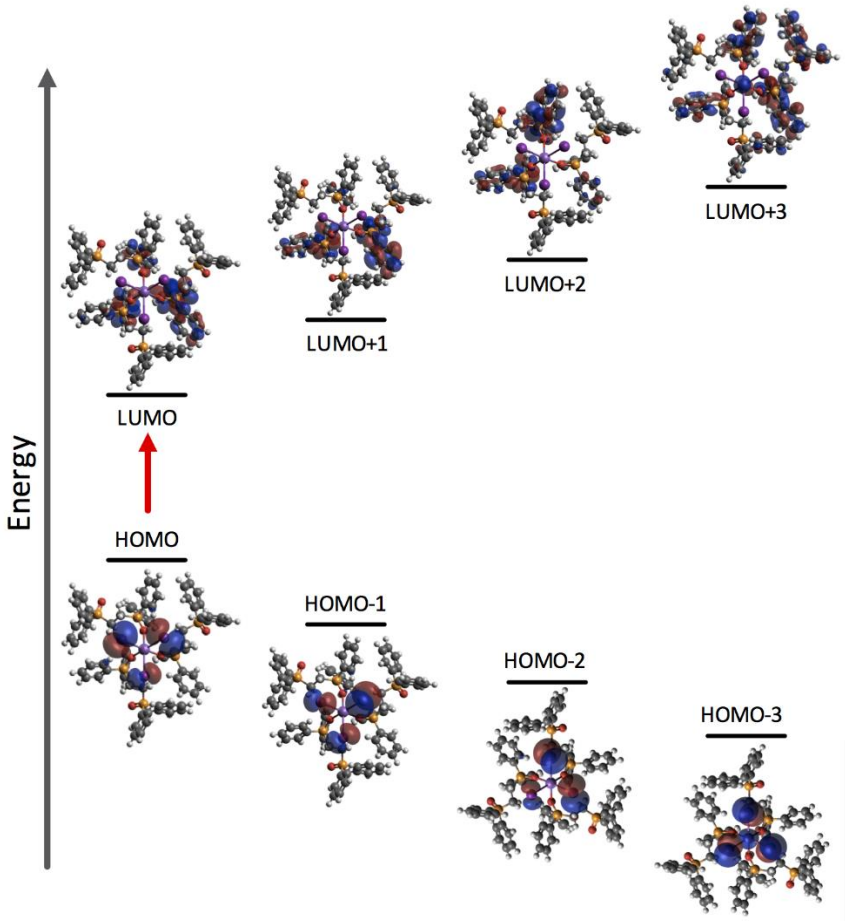

MO calculations indicate that an X/MLCT transition would constitute promotion of an electron from the HOMO-3 to the LUMO, while an XLCT would originate from the HOMO to the LUMO. The high energy separation (Table 3) between the HOMO-3 and the LUMO (4.05 eV) make this transition unlikely, leaving the XLCT as the most probable transition. TD-DFT calculations support this assertion by predicting that the lowest excited state results from electron transfer from the HOMO to the LUMO. The calculated transition energy of 3.54 eV indicates that **1** is a semi-conductive material with a band gap energy slightly larger than that of TiO_2 (3.2 eV) [43],[44]. The TD-DFT calculated UV-vis spectrum (Figure 7) also agrees with this interpretation, and shows that promotion of valence band electrons to the conduction band occurs well into the UV range, with a small portion extending into the visible region.

Figure 7. TD-DFT calculated UV-vis spectrum of $BiI_3(DppeO_2)_3$.

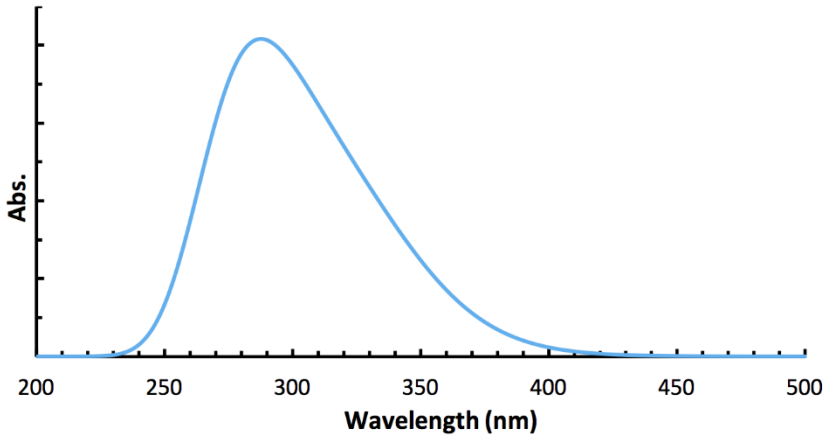

Conclusions:

Coordination of BiI_3 with ethane-1,2-diylbis(diphenylphosphane oxide) ($DppeO_2$) produces a metal-organic network complex $BiI_3(DppeO_2)_{3/2}$ (**1**). X-ray structural solution shows trigonal symmetry with a three-fold rotational position at bismuth and the inversion center located at the center of the $DppeO_2$ ligand. The resulting sheet network is nearly planar and consists of distorted octahedral *fac*-BiI_3O_3 centers linked by groups of three $DppeO_2$ ligands. Thermal analysis of the compound shows loss of all

ligands beginning near 300 °C. TD-DFT calculations reveal an XLCT electronic transition whereby electrons are excited from the I 5p HOMO to the $DppeO_2$ π*. These calculations predict a bandgap between the HOMO and LUMO of 3.54 eV, well within the range of current Bi(III) semiconductive materials.

Supplementary Material: Crystallographic information on CCDC 1588714 can be obtained free of charge by e-mailing data_request@ccdc.cam.ac.uk or by contacting The Cambridge Crystallographic Data Centre, 12 Union Road, Cambridge, CB2 1EZ UK; Fax +44(0)1223-336033; www.ccdc.cam.ac.uk/data_request/cif.

Acknowledgements. X-ray equipment was obtained with support from the NSF (CHE-0443345) and the College of William and Mary. The HHP group thanks the University of Maine Advanced Computing Group for their support and generous allocation of computing resources.

References:

(1) Y. Lei, G. Wang, S. Song, W. Fan, M. Pang, J. Tang, H. Zhang, Dalton Trans. 39, 3273–3278 (2010).
(2) X. Chang, J. Huang, C. Cheng, Q. Sui, W. Sha, G. Ji, S. Deng, G. Yu, Catal. Commun. 11, 460–464 (2010).
(3) Y. Wang, K. Deng, L. Zhang, J. Phys. Chem. C 114, 14300–14308 (2011).
(4) N.T. Hahn, S. Hoang, J.L. Self, C.B. Mullins, ACS Nano 6, 7712–7722 (2012).
(5) X. Zhang, Z. Ai, F. Jia, L. Zhang, J. Phys. Chem. C 112, 747–753 (2008).
(6) J.C. Ahern, R. Fairchild, J.S. Thomas, J. Carr, H.H. Patterson, Appl. Catal. B Environ. 179, 229–238 (2015).
(7) G.A. Fisher, N.C. Norman, Adv. Inorg. Chem. 41, 233–271 (1994).
(8) N. Mercier, N. Louvain, W. Bi, CrystEngComm 11, 710–734 (2009).
(9) L.-M. Wu, X.-T. Wu, L. Chen, Coord. Chem. Rev. 253, 2787–2804 (2009).
(10) S.A. Adonin, M.N. Sokolov, V.P. Fedin, Coord. Chem. Rev. 312, 1–21 (2016).
(11) F. Lazarini, S. Milicev, Acta Crystallogr., Sect. B 32, 2873–2875 (1976).
(12) W. Clegg, L.I. Farrugia, A. McCamley, N.C. Norman, A.G. Orpen, N.L. Pickett, S.E. Stratford, J. Chem. Soc., Dalton Trans. 2579–2587 (1993).
(13) P.G. Jones, D. Henschel, A. Weitze, A. Blaschette, Z. Anorg. Allg. Chem. 620, 1037–1040 (1994).
(14) C.J. Carmelt, L.I.Farrugia, N.C. Norman, J. Chem. Soc., Dalton Trans. 443–454 (1996).
(15) C.J. Carmalt, W. Clegg, M.R.J. Elsegood, R.J. Errington, J. Havelock, P. Lightfoot, N.C. Norman, A.J, Scott, Inorg. Chem. 35, 3709–3712 (1996).
(16) J.R. Eveland, K.H. Whitmire, Inorg. Chim. Acta 249, 41–46 (1996).

(17) G.A. Bowmaker, J.M. Harrowfield, P.C. Junk, B.W. Skelton, A.H. White, Aust. J. Chem. 51, 285–291 (1998).
(18) D. Mansfeld, M. Mehring, M. Schürmann, Inorg. Chim. Acta 348, 82–90 (2003).
(19) D. Mansfeld, C. Dietz, T. Rüffer, P. Ecorchard, C. Georgi, H. Lang, M. Schürmann, K. Jurkschat, M. Mehring, Main Group Met. Chem. 36, 193–208 (2013).
(20) A.N. Usoltsev, S.A. Adonin, P.A. Abramov, I.V. Korolkov, I.V. Yushina, O.V. Antonova, M.N. Sokolov, V.P. Fedin, Inorg. Chim. Acta 462, 323–328 (2017*)*.
(21) S.A. Adonin, M.I. Rakhmanova, D.G. Samsonenko, M.N. Sokolov, V.P. Fedin, Inorg. Chim. Acta 450, 232–235 (2016).
(22) M.A. Tershansy, A.M. Goforth, J.R. Gardinier, M.D. Smith, L. Peterson, H.-C. zur Loye, Solid State Sci. 9, 410–420 (2007).
(23) A.W. Kelly, A.M Wheaton, A.D. Nicholas, F.H. Barnes, H.H. Patterson, R.D. Pike, Eur. J. Inorg. Chem. 4990–5000 (2017).
(24) F. Marchetti, C. Pettinari, A. Pizzabiocca, A.A. Drozdov, S.I. Troyanov, C.O. Zhuravlev, S.N. Semenov, Y.A. Belousov, I.G. Timokhin, Inorg. Chim. Acta 363, 4038–4047 (2010).
(25) *SAINT PLUS*: Bruker Analytical X-ray Systems: Madison, WI, 2001.
(26) *SADABS*: Bruker Analytical X-ray Systems: Madison, WI, 2001.
(27) G.M. Sheldrick, Acta Crystallogr., Sect. A 64: 112−122 (2008).
(28) C.B. Hübschle, G.M. Sheldrick, B. Dittick, J. Appl. Cryst. 44, 1281−1284 (2011).
(29) A.D. Becke, J. Chem. Phys. 9, 5648–5652 (1993).
(30) C. Lee, W. Yang, R.G. Parr, Phys. Rev. B 37, 785–789 (1988).
(31) P.Fuentealba, H. Preuss, H. Stoll, L. Von Szentpály, Chem. Phys. Lett. 89, 418–422 (1982).
(32) Gaussian 09, Revision C.01, M.J. Frisch, G.W. Trucks, H.B. Schlegel, G.E. Scuseria, M.A. Robb, J.R. Cheeseman, G. Scalmani, V. Barone, B. Mennucci, G.A. Petersson, H. Nakatsuji, M. Caricato, X. Li, H.P. Hratchian, A.F. Izmaylov, J. Bloino, G. Zheng, J.L. Sonnenberg, M. Hada, M. Ehara, K. Toyota, R. Fukuda, J. Hasegawa, M. Ishida, T. Nakajima, Y. Honda, O. Kitao, H. Nakai, T. Vreven, J.A. Montgomery, Jr., J.E. Peralta, F. Ogliaro, M. Bearpark, J.J. Heyd, E. Brothers, K.N. Kudin, V.N. Staroverov, T. Keith, R. Kobayashi, J. Normand, K. Raghavachari, A. Rendell, J. C. Burant, S.S. Iyengar, J. Tomasi, M. Cossi, N. Rega, J.M. Millam, M. Klene, J.E. Knox, J.B. Cross, V. Bakken, C. Adamo, J. Jaramillo, R. Gomperts, R.E. Stratmann, O. Yazyev, A.J. Austin, R. Cammi, C. Pomelli, J.W. Ochterski, R.L. Martin, K. Morokuma, V.G. Zakrzewski, G.A. Voth, P. Salvador, J.J. Dannenberg, S. Dapprich, A.D. Daniels, O. Farkas, J.B. Foresman, J.V. Ortiz, J. Cioslowski, D.J. Fox, Gaussian, Inc., Wallingford CT, 2010.
(33) R. Bauernschmitt, R. Ahlrichs, Chem. Phys. Lett. 256, 454–464 (1996).
(34) R.E. Stratmann, G.E. Scuseria, M.J. Frisch, J. Chem. Phys. 109, 8218–8224 (1998).
(35) M.E. Casida, C. Jamorski, K.C. Casida, D.R. Salahub, J. Chem. Phys. 108, 4439–4449 (1998).
(36) M.D. Hanwell, D.E. Curtis, D.C. Lonie, T. Vandermeersch, E. Zurek, G.R.J. Hutchison, Cheminform 4, 17 (2012).
(37) Y.J. Wang, L. Xu, J. Mol. Struct. 875, 570–576 (2008).
(38) Y.H. Peng, S.F. Sun, Inorg. Chem. Commun. 22, 29–32 (2012).
(39) A.B. Maurer, K. Hu, G.J. Meyer, J. Am. Chem. Soc. 139, 8066−8069 (2017).

(40) H.A. Evans, J.G. Labram, S.R. Smock, G. Wu, M.L. Chabinyc, R. Seshadri, F. Wudl, Inorg. Chem. 56, 395−401 (2017).
(41) X. Huang, S. Huang, P. Biswas, R. Mishra, J. Phys. Chem. C 120, 28924−28932 (2016).
(42) A.C. Wibowo, M.D. Smith, H.-C. zur Loye, Cryst. Growth Des. 11, 4449–4457 (2011).
(43) C. Dette, M.A. Pérez-Osorio, C.S. Kley, P. Punke, C.E. Patrick, P. Jacobson, F. Giustino, S.J. Jung, K. Kern, Nano Lett. 14, 6533–6538 (2014).
(44) J. Tao, T. Luttrell, M.A. Batzill, Nat. Chem. 3, 296–300 (2011).

Table 1. Crystal and Structure Refinement Data.

	$BiI_3(DppeO_2)_{3/2}$, (**1**)
CCDC deposit no.	1588714
color and habit	orange block
size, mm	0.31 × 0.30 × 0.18
Formula	$C_{39}H_{36}Bi_1I_3O_3P_3$
formula weight	1235.26
space group	*R*–3*c*
a Å	14.7907(9)
c, Å	63.920(4)
volume, Å^3	12110.0(16)
Z	12
ρ_{calc}, g cm^{-3}	2.033
F_{000}	6972
μ(Mo Kα), mm^{-1}	6.816
Radiation	MoKα (λ = 0.71073 Å)
temperature, K	100
residuals:[a] R; R_w	0.0167, 0.0445
goodness of fit	1.037
peak and hole, eÅ^{-3}	0.751, −0.877

[a] $R = R_1 = \Sigma||F_o| - |F_c||/\Sigma|F_o|$ for observed data only. $R_w = wR_2 = \{\Sigma[w(F_o^2 - F_c^2)^2]/\Sigma[w(F_o^2)^2]\}^{1/2}$ for all data.

Table 2. Bond length (Å) and angle (°) comparison of DFT and X-ray parameters for **1**.

Parameter	Calculated	X-ray
Bi–I	3.152	2.942
Bi–O	2.354	2.458
I–Bi–I	93.3	95.5
O–Bi–I	89.2	84.5
Bi–O–P	154	156

Table 3. Calculated MO energies and composition for **1**.

MO	Energy	Composition
LUMO+3	–1.265	Bi 6s / $DppeO_2$ π^*
LUMO+2	–1.311	$DppeO_2$ π^*
LUMO+1	–1.341	$DppeO_2$ π^*
LUMO	–1.407	$DppeO_2$ π^*
HOMO	–5.357	I 5p
HOMO–1	–5.392	I 5p
HOMO–2	–5.425	I 5p
HOMO–3	–5.461	Bi 6s / I 5p